



## OPEN Risk factor analysis and prediction model to establish recurrence or progression of non-functioning pituitary adenomas in men after transnasal sphenoidal surgery

Jiansheng Zhong<sup>1,5</sup>, Yuyang Chen<sup>1,5</sup>, Mingyue Wang<sup>2</sup>, Jun Li<sup>1,3</sup>, Ziqi Li<sup>1</sup>, Haixiang Li<sup>4</sup>, Liangfeng Wei<sup>1,3</sup> & Shousen Wang<sup>1,3,4</sup>✉

This paper aims to analyze the risk factors for the recurrence or progression of non-functioning pituitary adenomas (NFPAs) in male patients after transnasal sphenoidal surgery and to develop a predictive model for prognosis. Clinical and follow-up data of 126 male patients with NFPAs treated by transnasal sphenoidal surgery from January 2011 to January 2021 in Fuzhou 900th Hospital were retrospectively analyzed. Lasso regression analysis was used to screen the best predictors, and the predictors were further screened by multivariate logistic regression analysis, and the nomogram prediction model was constructed. The performance of the model was verified by three aspects: discrimination, calibration and clinical utility by using the consistency index (C-index), receiver operating characteristic curve (ROC), calibration curve, clinical decision curve (DCA) and Clinical impact curve (CIC). Out of 126 cases, 7 (5.56%) showed postoperative tumor recurrence, and 18 (14.29%) exhibited postoperative residual regrowth (progression). Age ( $P = 0.024$ ), maximum tumor diameter ( $P < 0.001$ ), modified Knosp grade ( $P < 0.001$ ), resection extent ( $P < 0.001$ ), Ki67 ( $P < 0.001$ ), pressure symptom ( $P < 0.001$ ), Pre-op hypopituitarism ( $P = 0.048$ ), Post-op new hypopituitarism ( $P = 0.017$ ) showed significant differences among the recurrence group, the progression group, and the alleviation group. Three independent risk factors (Ki67, modified Knosp grade, and resection extent) affecting postoperative remission were used to construct a predictive model for long-term postoperative failure to remit. The C-index of the nomogram model was 0.823, suggesting that the model had a high discriminatory power, and the AUC of the area under the ROC curve was 0.9[95% CI (0.843, 0.958)]. A nomogram prediction model based on modified Knosp grading (grades 3B-4), resection extent (partial resection), and Ki-67 ( $\geq 3\%$ ) predicts the recurrence or progression of NFPAs in men after transnasal sphenoidal surgery.

**Keywords** Pituitary adenoma, Male patients with pituitary adenoma, Tumor recurrence or progression, Transnasal sphenoidal surgery, Nomogram, Prognostic models

Pituitary adenoma (PA) is one of the most common benign intracranial tumors, accounting for 10–20% of all primary intracranial tumors<sup>1,2</sup>, and the nonfunctioning subtype accounts for 15–30% of the total<sup>3</sup>. In general, the main characteristic of non-functioning pituitary adenomas (NFPAs) is that they are not accompanied by clinical symptoms induced by hormonal abnormalities, and these tumours tend to increase in size progressively, leading to a series of secondary manifestations, including headaches, visual disturbances, limitation of visual field range, and subsequent hypopituitarism<sup>4</sup>. Tumors with a maximum diameter of  $\geq 4$  cm are referred to as giant PAs, and tumors with a maximum diameter of  $\geq 3$  cm are called as large PAs<sup>5–7</sup>. Surgery is usually the first-line treatment for large NFPAs<sup>8</sup>. Regardless of whether the surgery is performed through a transnasal butterfly or

<sup>1</sup>Fujian Medical University, Fuzong Clinical Medical College of Fujian Medical University, Fuzhou 900 Hospital, Fuzhou, China. <sup>2</sup>Department of Pathology, Fuzhou 900 Hospital, Fuzhou, China. <sup>3</sup>Fujian Provincial Clinical Medical Research Center for Minimally Invasive Diagnosis and Treatment of Neurovascular Diseases, Fuzhou, China. <sup>4</sup>Department of Neurosurgery, Dongfang Hospital, Xiamen University, Fuzhou, China. <sup>5</sup>These authors contributed equally: Jiansheng Zhong and Yuyang Chen. ✉email: wshsen1965@fjmu.edu.cn

transcranial approach, the results are unsatisfactory. Extra-saddle residual tissue are reported in 53% of cases at 5 years and in more than 80% of cases at 10 years<sup>9</sup>. Even in the case of complete surgical resection, the 10-year long-term recurrence rate is high, about 7–12%<sup>9,10</sup>.

Currently, nomogram prediction models are widely used to predict clinical outcomes in diseases such as tumors and neurodegenerative disorders<sup>11,12</sup>. However, studies using nomogram prediction models to explore the effect on postoperative outcomes after the transnasal sphenoidal surgery approach for NFPA in men have not yet been reported. Female patients with NFPA have a higher incidence of diabetes mellitus type 2, myocardial infarction, cerebral infarction, and fracture compared with males<sup>13–15</sup>, and these conditions may influence the postoperative outcomes. Therefore, female patients are excluded from this study, which aims to investigate the factors influencing the outcome after transnasal sphenoidal surgery approach for NFPA in males and to develop a nomogram model to predict tumor recurrence or progression.

## Methods

### General information

The clinical data of 243 male patients with PA who underwent microscopic surgery via the transnasal sphenoidal surgery approach at Fuzhou 900th Hospital from January 2011 to December 2021 were retrospectively analyzed and performed by the same senior neurosurgeon. The cut-off date for follow-up was 1 January 2024 for all patients. A total of 126 patients met the inclusion criteria and comprised the cohort. Inclusion criteria were as follows: (1) Patients with a clinical diagnosis of NFPA in the absence of any pituitary hormone hypersecretion and hormonal symptoms and an immunohistochemically confirmed NFPA (silent gonadotropin cell adenoma, adrenocorticotropin cell adenoma, PIT1 gene spectrum, and null cell tumor) according to the 2017 WHO classification criteria for PAs<sup>16</sup>; (2) those who were older than 18 years; (3) those who had complete medical records; and (4) those who had complete imaging data and underwent pituitary thin-layer MRI examination using a 3.0T magnetic resonance scanner at our hospital. Exclusion criteria were as follows: (1) those who were not treated by microscopic surgery through the transnasal sphenoidal surgery approach (excluded 38 patients), (2) those who had a history of craniofacial surgery and sellar region surgery (excluded 21 patients), (3) those who had incomplete postoperative relevant data or lost visits (excluded 34 patients), (4) those who had been treated by radiotherapy and medication (excluded 19 patients), (5) those who had combined with other intracranial tumours, malignant tumours (excluded 5 patients). Patients were reviewed at 3, 6 and 12 months postoperatively and annually thereafter (including hormones and pituitary MRI) for a minimum of 2 years. Pituitary images were evaluated by neurosurgeon W and neuroradiologist L during the follow-up period. Residual tumor was defined as tissue with the same MRI features as before tumor resection, confined to the area where the tumor was found preoperatively, and could not be a normal structure or implant material<sup>17</sup>. For patients with residual tumor, the maximum residual tumor diameter was measured on the first postoperative MRI, the presence of residual tumor growth (progression) was assessed on subsequent MRIs, and any increase in tumor size in any dimension was assessed as residual tumor growth<sup>17</sup>. Recurrence was defined as the absence of residual tumor during the follow-up period when MRI revealed the appearance of a new mass<sup>17</sup>. Therefore, we divided the group into recurrence (tumour re-growth after GTR), progression (tumour re-growth after STR) and alleviation (no tumour growth detected after surgery). Follow-up was conducted by telephone and outpatient or inpatient review.

All procedures included in the study were approved by the Clinical Medical Ethics Committee of the Fuzhou 900th Hospital. All patients or their families provided written informed consent for the clinical procedures used and for inclusion in the study. All methods in the study were performed in accordance with relevant guidelines and regulations.

### Data acquisition

① General information, including the patient's age, follow-up time; ② Clinical symptoms, including headaches, vision problems and visual field changes; ③ Imaging data, including maximum tumor diameter (MPAD), modified Knosp grade (The Knosp grading system is used to assess the extent of lateral extension of the adenoma into the cavernous sinus on both sides, and the modified Knosp grading includes the differentiation between grades 3 A and 3B infiltration of the upper or lower cavernous sinus compartment<sup>18</sup>), resection rate (Tumor resection was assessed based on the MRI performance at 3 months postoperatively, distinguishing between gross total resection [GTR] i.e. >60% of the resection area and subtotal resection [STR] i.e. ≤60% of the resection area using the Hoffman classification system<sup>19</sup>), presence of stroke, and cystic change; ④ Pathology data, including Ki67 (Pathological reports showed Ki7 indices divided into low-level [ $<3\%$ ] group and high-level [ $\geq 3\%$ ] group<sup>20</sup>); ⑤ Biochemical indices, including preoperative, 1 week postoperative, and 3 months postoperative growth hormone (GH), thyroid stimulating hormone (TSH), adrenocorticotropin hormone (ACTH), prolactin (PRL), follicle stimulating hormone (FSH), luteinising hormone (LH), free thyroxine (FT4), insulin like growth factor-1 (IGF-1), testosterone (TE) and cortisol (COR). All hormone tests were performed by using chemiluminescence detection methods with the Siemens ADVIA Centaur XP machine. Male reference values for each hormone were as follows: < 2 ng/ml GH, 0.35–5.5 mIU/ml TSH, 1.4–18.1 mIU/ml FSH, 1.5–9.3 mIU/ml LH, 2.1–17.7  $\mu\text{g/L}$  PRL, 4.7–48.8 ng/ml ACTH, 175–781 nmol/L TE, 4.2–24.8  $\mu\text{g/dl}$  8:00 am COR and Changes in IGF-1 normal range with age (Appendix 1)<sup>21</sup>.

### Statistical processing

The data obtained from the study were analyzed using SPSS 27.0 statistical software. Measured data were expressed as mean  $\pm$  standard deviation for normal distribution, t-test for comparison between two groups, ANOVA for comparison of count data between multiple groups, and Bonferroni test for two-by-two comparisons; correlation analyses were performed using Pearson's correlation test; data that did not conform to normal distribution were expressed as median [quartile], and Mann–Whitney U-test for comparison between two groups, Kruskal–Wallis

test for multigroup comparison, and Nemenyi test for two-by-two comparisons between multiple groups. Count data were expressed as the number of cases (n%), and comparisons between two groups were evaluated using the chi-square, corrected chi-square, or Fisher's exact probability method, and differences were considered statistically significant at  $P < 0.05$ .

### Immunohistochemical analysis

The Ki67 index was expressed as the percentage of Ki67-immunoreactive cells out of at least 500 tumor cells counted in the highest labelled area ("hotspot"). After the automated scoring of the staining of the samples using Image J software, the Trainable Weka Segmentation plug-in was then used to count the positive and negative cells separately.

### Model construction and validation

The predictors of postoperative recurrence or progression were screened by LASSO regression analysis and on this basis were further determined using multifactorial logistic regression analysis. Then, R software was used to construct the prediction model of the nomogram. The internal validation of the prediction model was performed by repeated sampling 1000 times using the Bootstrap method, calculating the consistency index (C-index), plotting the working curve (ROC) of the subjects, and calculating the area under the curve (AUC), to verify the discriminatory degree of the model. The Hosmer–Lemeshow method was used to assess the goodness-of-fit of the model, and calibration curves were plotted to verify the calibration of the model. Clinical decision curve (DCA) was plotted to evaluate the clinical utility of the model. Finally, clinical impact curves (CIC) were plotted to assess the clinical usefulness and applicability of the model with the best diagnostic value.

## Results

### Comparison of general clinical data

A total of 126 male patients with NFPA were included, with a mean age of  $50.3 \pm 13.50$  (18–74) years and a mean tumour diameter of  $33.12 \pm 11.99$  (12.99–80.35) mm. We classified patients with 76 (60.3%) low Modified Knosp grade (0–3 A) and 50 (39.7%) patients with high Modified Knosp grade (3B–4) on the basis of parasellar extension of NFPA. Based on 3-month postoperative imaging data, GTR and STR were achieved in 89 (70.6%) and 37 (28.1%) of patients, respectively. A total of 102 (80.95%) patients experienced varying degrees of pressure symptoms (headache, vision loss and visual field defects, etc.). The longest follow-up was 153 months and the shortest was 28 months, with a median follow-up of 94.5 (58–118.75) months. The median time to recurrence was 56 (12–68) months in the recurrence group and 19.5 (6–31.25) months in the progression group. Hypopituitarism was detected preoperatively in 59 patients (hypoadrenalism 24, hypothyroidism 20, hypogonadism 33, GH deficiency 24) when hormone levels were analysed. After tumour resection, 46 patients (hypoadrenalism 9, hypothyroidism 26, hypogonadism 19, GH deficiency 13) developed new-onset hypopituitarism. Normalisation of the hormonal axis in 14 patients after surgery. In the univariate analysis of the postoperative outcomes of 126 patients, 7 cases of postoperative recurrence (5.56%), and 18 cases of postoperative residual regrowth (14.29%). Age, MPAD, tumor type, resection extent, modified Knosp grading, Ki-67 index, pressure symptoms, Pre-op hypopituitarism, Post-op new hypopituitarism, FSH levels 7 days before operation, TSH levels 7 days before and 3 months after operation, and Prolactin levels 7 days and 3 months after operation significantly differed among the recurrence, progression, and alleviation groups. Patient characteristics and hormonal results are detailed in Tables 1 and 2.

### Selection of risk predictors and multifactor analysis

Postoperative outcomes (recurrence or progression and alleviation) were the dependent variables, and 17 variables were included (Fig. 1). Due to the correlation between different independent variables, the model was downscaled, the most representative predictors of postoperative recurrence or progression of NFPA in men were selected, and LASSO regression analyses were performed on all independent variables. With the change of the penalty coefficient  $\lambda$ , the variables initially included in the model were gradually reduced, and the minimum error  $\lambda + 1$  (0.129) in the 10-fold cross-validation method was finally selected as the optimal value (Fig. 1A). Ki67, tumor type, modified Knosp grade, and resection extent were finally selected as the independent variables for predicting postoperative recurrence or progression (Fig. 1B). These four independent variables were further incorporated into a logistic regression model, and the results showed that Ki67, Modified Knosp grade, and resection extent were the predictors of postoperative recurrence or progression of NFPA in men ( $P < 0.05$ , Fig. 2).

### Construction of a predictive model for nomogram

The predictors selected from the above multifactor logistic regression analyses were incorporated into the nomogram prediction model. In the figure, the corresponding scores were obtained by projecting the values of each predictor upward to the scale at the top of the nomogram. Subsequently, the scales of all independent predictors were summed to obtain the total score, and the predictive value of postoperative recurrence or progression of NFPA in male patients was obtained (Fig. 3).

### Evaluation of the effects of nomogram

The internal validation of the nomogram prediction model using the bootstrap method with a self-sampling number of 1000 showed that the C-index of the nomogram model was 0.823, the AUC of the area under the ROC curve was 0.9 [95% CI (0.843–0.958)], the sensitivity was 92%, and the specificity was 72.3% (Fig. 4). The calibration curves of the nomogram plots showed that the predictions agreed with the observations, and the Hosmer–Lemeshow goodness-of-fit test indicated that the model aligned with the observed data (Fig. 5). In addition, the DCA decision curve revealed that the model had a significant positive net benefit and good clinical

Factors	Recurrence (n=7)	Progression (n=18)	Alleviation (n=101)	F/H/ $\chi^2$	P
Age (year)	47.00 ± 16.26	40.50 ± 14.58	52.00 ± 12.56	7.486	0.024
MPAD (mm)	45.68 ± 16.71	44.95 ± 11.37	29.23 ± 9.54	28.194	<0.001
Tumour type					
Macroadenomas	1(0.79%)	6(4.76%)	87(69.05%)	36.716	<0.001
Giant adenomas	6(4.76%)	12(9.52%)	14(11.11%)		
Resection extent					
GTR	7(5.56%)	0(0.00%)	82(65.08%)	51.630	<0.001
STR	0(0.00%)	18(14.29%)	19(15.08%)		
Modified Knosp grade					
0-3A	0(0.00%)	4(3.17%)	75(59.52%)	30.145	<0.001
3B-4	7(5.56%)	14(11.11%)	26(20.63%)		
Ki-67					
<3%	6(4.76%)	8(6.35%)	88(69.84%)	18.16	<0.001
≥3%	1(0.79%)	10(7.94%)	13(10.32%)		
Cystic change					
Yes	1(0.79%)	5(3.97%)	22(17.46%)	0.588	0.745
No	6(4.76%)	13(10.32%)	79(62.70%)		
Pituitary apoplexy					
Yes	1(0.79%)	4(3.17%)	25(19.84%)	0.425	0.809
No	6(4.76%)	14(11.11%)	76(60.32%)		
Pressure symptom					
Yes	5(3.97%)	11(8.73%)	86(68.25%)	134.258	<0.001
No	2(1.59%)	7(5.56%)	15(11.90%)		
Pre-op hypopituitarism					
Yes	4(3.17%)	13(10.32%)	59(46.83%)	6.076	0.048
No	3(2.38%)	5(3.97%)	42(33.33%)		
Post-op new hypopituitarism					
Yes	1(0.79%)	2(1.59%)	43(34.13%)	8.103	0.017
No	6(4.76%)	16(12.70%)	58(46.03%)		
Follow-up time (M)	115 (100.5-132.5)	109 (81.25-135.75)	90 (55-115)	5.546	0.062
Reoperation time (M)	56 (12-68)	19.5 (6-31.25)	-	- 1.878	0.060

**Table 1.** Comparison of patient characteristic variables among the 3 groups.  $P < 0.05$  statistically significant. F-value: is a test statistic in analysis of variance (ANOVA) that measures the relative magnitude of the difference in means between groups compared to the difference in means within groups. H-value: the test statistic of the Kruskal-Wallis test, which measures the dispersion of the rank sum of multiple samples.  $\chi^2$ -value: a statistic calculated when performing a chi-square test to assess the significance of the difference between the observed frequencies and the expected frequencies. Abbreviations: MPAD: Maximum tumour diameter; GTR: gross total resection; STR: subtotal resection; M: month.

utility in predicting recurrence of NFPA in men (Fig. 6). The CIC intuitively showed that the nomograms had a superior overall net benefit and a greater impact on patient prognosis over a broad and practical range of threshold probabilities, suggesting that the model has significant predictive value (Fig. 7).

### Analysis of immunohistochemical results

Of the 25 patients with recurrence or progression, 12 (48%) underwent a second operation, where the postoperative Ki67 index of the second operation in 9 (75%) of these patients was elevated compared with the first; 7 (77.78%) went from the low-level (<3%) group to the high-level group (≥3%), but the Ki67 index was still <20% (Fig. 8).

### Discussion

The aim of this study was to construct a nomogram model for predicting long-term outcomes after trans sphenoidal surgery in male NFPA patients using pre- and postoperative imaging and clinical data. The predictive model ultimately incorporated 3 predictors: Ki67, Modified Knosp grade, and resection extent. The ROC curvilinear area under the model AUC=0.9, 95% CI (0.843~0.958), suggesting that the model has a good predictive effect. The internal validation of the constructed model showed that the model had good discrimination and calibration, which could help clinicians predict the postoperative remission and guide the development of individualised follow-up plans and treatment protocols.

Hormone	Time	Recurrence (n = 7)	Progression (n = 18)	Alleviation (n = 101)	F	P
GH, ng/mL	Preoperative day 7	0.88 ± 1.42	0.40 ± 0.60	0.84 ± 3.13	0.187	0.300
	Postoperative day 7	0.58 ± 1.04	0.39 ± 0.36	0.59 ± 2.41	0.667	0.515
	Postoperative month 3	0.45 ± 0.54	0.40 ± 1.03	0.57 ± 3.13	0.048	0.953
ACTH, ng/mL	Preoperative day 7	25.17 ± 11.64	18.68 ± 16.07	45.14 ± 148.28	0.345	0.709
	Postoperative day 7	20.59 ± 14.93	14.89 ± 20.15	40.84 ± 148.46	0.335	0.716
	Postoperative month 3	48.18 ± 71.86	22.09 ± 15.50	30.90 ± 44.61	0.914	0.404
TSH, mIU/L	Preoperative day 7	1.99 ± 0.74	3.87 ± 6.51	1.87 ± 1.97 <sup>a</sup>	3.409	0.036
	Postoperative day 7	1.69 ± 2.23	2.34 ± 3.53	1.26 ± 2.02	1.718	0.184
	Postoperative month 3	2.03 ± 0.74	2.78 ± 1.67	1.92 ± 1.25 <sup>a</sup>	3.378	0.037
PRL, µg/L	Preoperative day 7	28.74 ± 24.98	173.22 ± 628.00	47.02 ± 326.45	0.894	0.412
	Postoperative day 7	11.97 ± 15.07	64.33 ± 201.44	7.66 ± 22.21 <sup>a</sup>	4.084	0.019
	Postoperative month 3	18.23 ± 24.97	87.22 ± 293.84	11.45 ± 51.84 <sup>a</sup>	3.105	0.048
FSH, mIU/ml	Preoperative day 7	9.16 ± 7.68	26.34 ± 53.75	8.98 ± 11.40 <sup>a</sup>	4.570	0.012
	Postoperative day 7	5.60 ± 4.15	9.06 ± 15.22	6.78 ± 12.28	0.304	0.738
	Postoperative month 3	7.18 ± 5.25	10.06 ± 19.29	7.47 ± 13.23	0.269	0.764
LH, mIU/ml	Preoperative day 7	3.50 ± 2.26	2.18 ± 1.67	2.94 ± 2.03	1.491	0.229
	Postoperative day 7	2.11 ± 1.44	2.93 ± 2.01	2.88 ± 2.64	0.743	0.478
	Postoperative month 3	4.44 ± 3.66	2.87 ± 1.83	3.21 ± 2.71	0.894	0.412
FT4, ng/dl	Preoperative day 7	11.82 ± 2.86	10.72 ± 3.54	12.49 ± 7.10	2.226	0.329
	Postoperative day 7	12.69 ± 3.05	10.79 ± 3.52	12.68 ± 9.44	4.12	0.127
	Postoperative month 3	13.30 ± 3.12	12.25 ± 3.27	14.06 ± 16.43	3.55	0.169
TE, ng/mL	Preoperative day 7	293.70 ± 265.48	184.02 ± 210.95	192.75 ± 146.94	1.411	0.494
	Postoperative day 7	118.06 ± 95.41	79.13 ± 61.59	101.98 ± 106.32	0.634	0.728
	Postoperative month 3	330.35 ± 289.71	206.73 ± 225.26	234.18 ± 193.40	1.629	0.443
IGF-1, ng/mL	Preoperative day 7	282.83 ± 263.54	116.30 ± 125.30	139.56 ± 155.90	1.983	0.371
	Postoperative day 7	216.53 ± 182.5	80.97 ± 74.94	124.11 ± 72.40	2.548	0.280
	Postoperative month 3	100.80 ± 57.33	85.36 ± 67.51	114.55 ± 66.48	4.113	0.128
COR, µg/mL	Preoperative day 7	9.45 ± 5.92	11.66 ± 13.53	11.02 ± 8.72	0.463	0.793
	Postoperative day 7	15.18 ± 15.04	24.97 ± 18.89	20.80 ± 15.58	1.985	0.371
	Postoperative month 3	9.40 ± 6.83	12.06 ± 6.49	10.11 ± 6.20	1.198	0.549

**Table 2.** Differences between pre- and postoperative pituitary hormone levels in all patients. <sup>a</sup> Comparison of progression and remission groups,  $P < 0.05$ .  $P < 0.05$  statistically significant. F-value: is a test statistic in analysis of variance (ANOVA) that measures the relative magnitude of the difference in means between groups compared to the difference in means within groups. Abbreviations: GH: growth hormone; ACTH: adrenocorticotropic hormone; TSH: thyroid-stimulating hormone; PRL: prolactin; FSH: follicle-stimulating hormone; LH: luteinizing hormone; FT4: free thyroxine; IGF-1: insulin like growth factor-1; TE: testosterone; COR: cortisol.

The prognosis of PA is generally assessed based on the imaging features and pathological findings<sup>22</sup>. Previous studies have shown that patients with NFPA have significantly lower remission rates than patients with functional PA and have a higher probability of recurrence or progression<sup>23–26</sup>. The recurrence or progression rate in patients with NFPA treated with surgery ranges from 15–66%<sup>10,27</sup>; the recurrence or progression rate peaks between 1 and 5 years after surgery and declines after 10 years<sup>23</sup>. The present study with a follow-up of 2–10 years yielded a recurrence or progression rate of 19.84% for men with NFPA, which agreed with the appellate literature. Interestingly, there was no significant difference in the comparison of follow-up time among the three groups in this study, but the time to reoperation was shorter in the progressive group compared to the recurrent group.

Tumor size and surgical resection extent are factors influencing tumor recurrence or progression<sup>17,28–30</sup>. Excessive tumor size reduces the likelihood of its complete resection and may affect prognosis and recurrence. Hofstetter<sup>6</sup> found that larger tumour diameters were most likely to have postoperative residuals. Chang<sup>31</sup> found that supratrochlear and/or cavernous sinus residuals commonly contributed to the progression of postoperative PA. In this study, the tumor MPAD was significantly greater in the recurrence or progression group than in the remission group, and GTR and STR were differentiated based on the postoperative imaging findings and surgical records using the Hoffman classification system<sup>19</sup> to derive a significantly higher rate of postoperative recurrence in the tumor STR group (48.65%) than in the GTR group (7.87%). NFPA was usually manifested in an inactive state; the onset of headache was observed only in the presence of a large tumor, visual field defects and other clinical symptoms were detected only when the tumor was large, and NFPA was prone to recurrence or progression at the residual site<sup>25,26</sup>. At the same time, surgery demonstrated extremely significant results in relieving compression symptoms, and all cases in this study experienced varying degrees of improvement

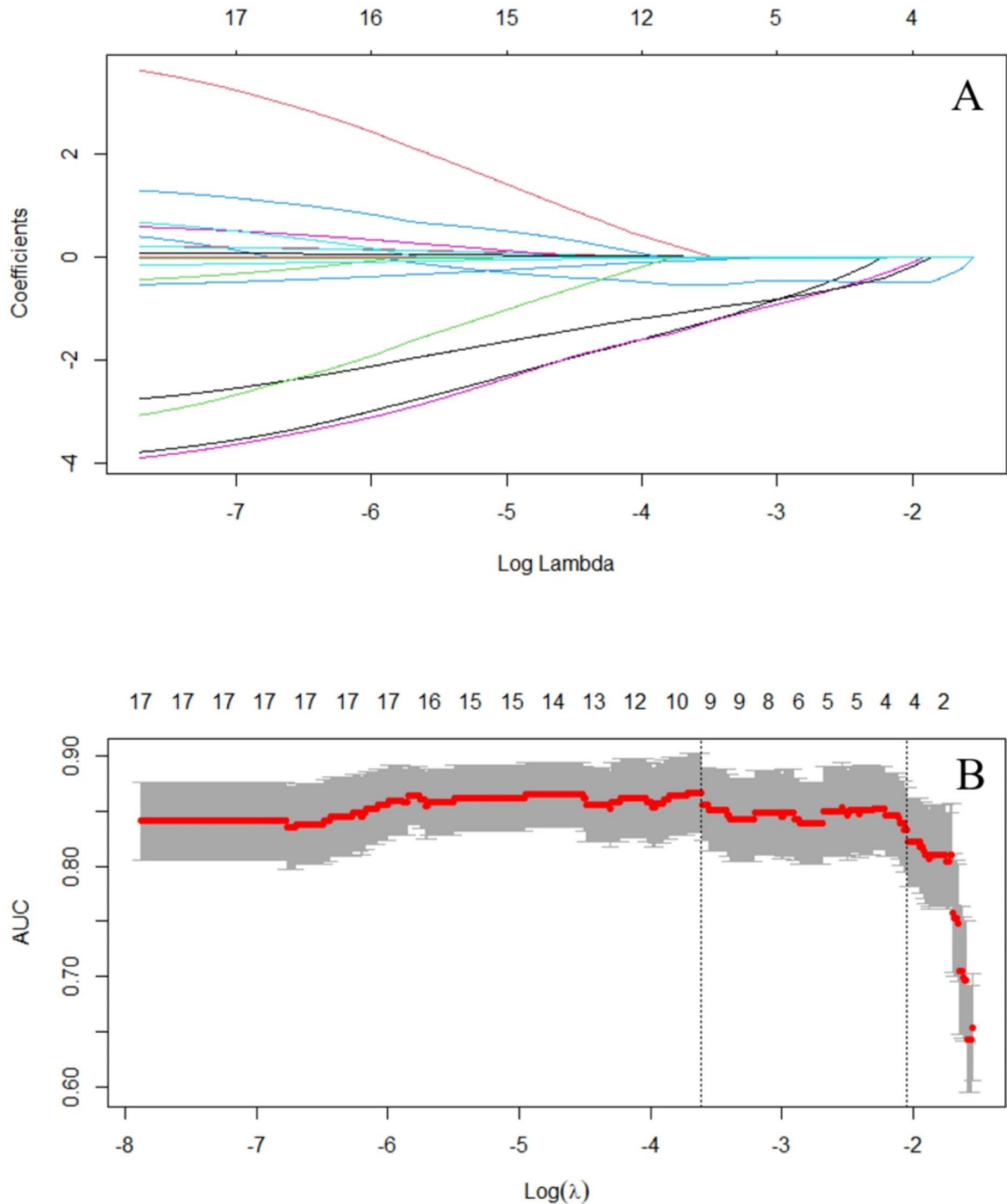


**Fig. 1.** The variables selection using the LASSO logistic regression model. **(A)** Coefficient curves of 17 clinical predictors. Lasso coefficient profiles of the features. A coefficient profile plot was produced against the log ( $\lambda$ ) sequence. **(B)** A vertical line was drawn at the value selected using tenfold cross-validation, where optimal values by using the minimum criteria and the 1 standard error of the minimum criteria. Note: The 17 variables included age, Ki67, whether cystic change, Pituitary apoplexy, tumour type, maximum diameter, Modified Knosp grade, resection rate, Pressure symptom, Pre-op hypopituitarism, Post-op new hypopituitarism, thyroid-stimulating hormone and free thyroxine at 7 days preoperatively, 7 days postoperatively and 3 months postoperatively.

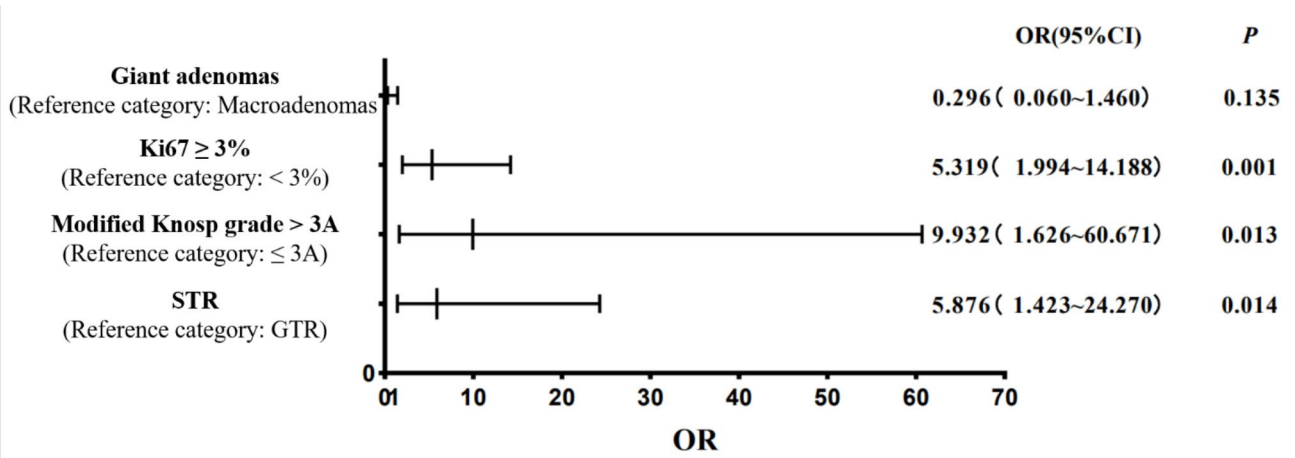


**Fig. 2.** Multifactorial logistic regression scores for predictors of recurrence or progression after transnasal sphenoidal surgery in men with NFPA. Abbreviations: NFPA: non-functioning pituitary adenomas; GTR: gross total resection (> 60% of the resection area); STR: subtotal resection (≤ 60% of the resection area). OR: Odds Ratio is the ratio ratio, also known as the dominance ratio and ratio ratio, is an indicator of the strength of the association between disease and exposure in case-control studies. 95% CI: is the 95% confidence interval for the OR value, indicating that there is a 95% confidence level that the true OR value will fall within this interval in multiple replicate samples.

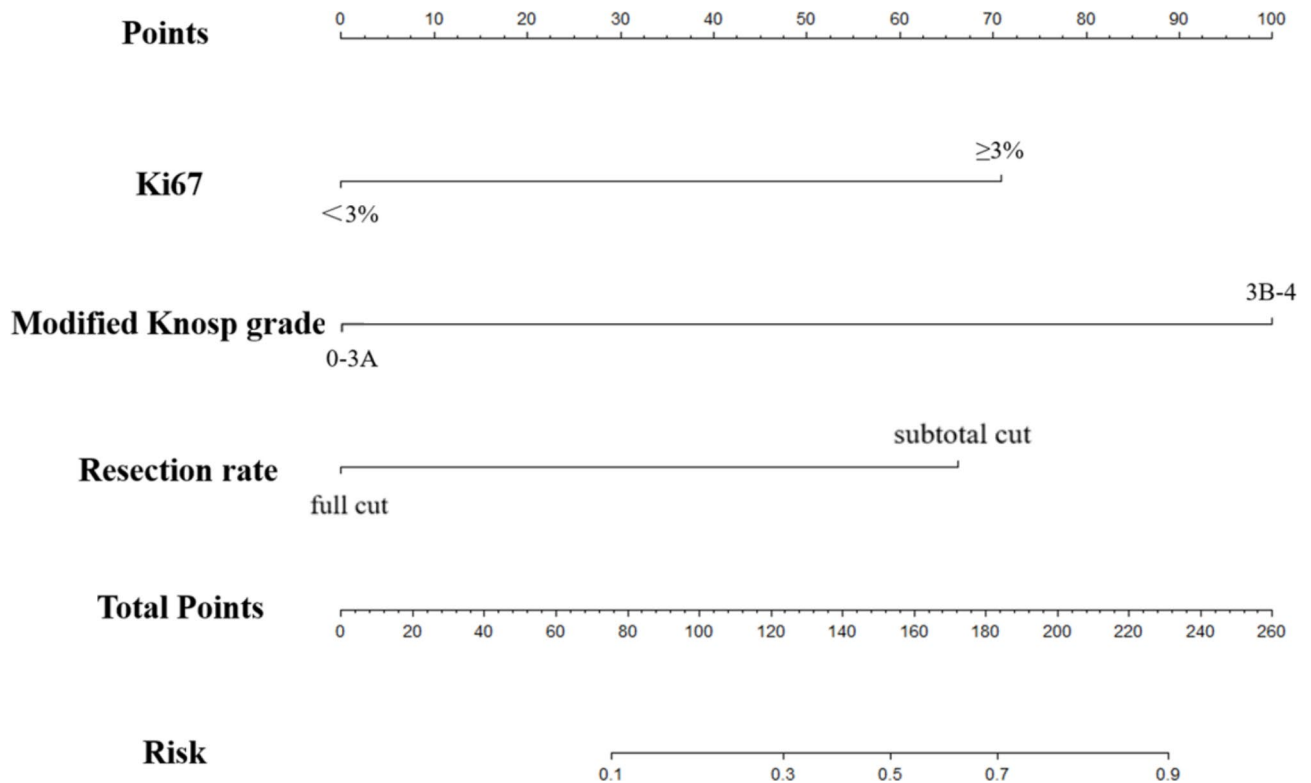


**Fig. 3.** Predicted nomogram of recurrence or progression of NFPA in men after transnasal sphenoidal surgery. The predictor points can be found on the uppermost point scale that correspond to each patient variable and can be added up. The total score predicted to the bottom scale indicates the risk of NFPA not being unrelieved. Abbreviations: NFPA: non-functioning pituitary adenomas.

in compression symptoms after surgery. Even with subsequent recurrence or progression of the disease, the compression symptoms were still significantly reduced compared to the state before the initial surgery. This phenomenon is most likely attributable to the enhanced postoperative follow-up management strategy and the effective reduction of tumour volume, both of which contributed to the significant improvement of the patients'

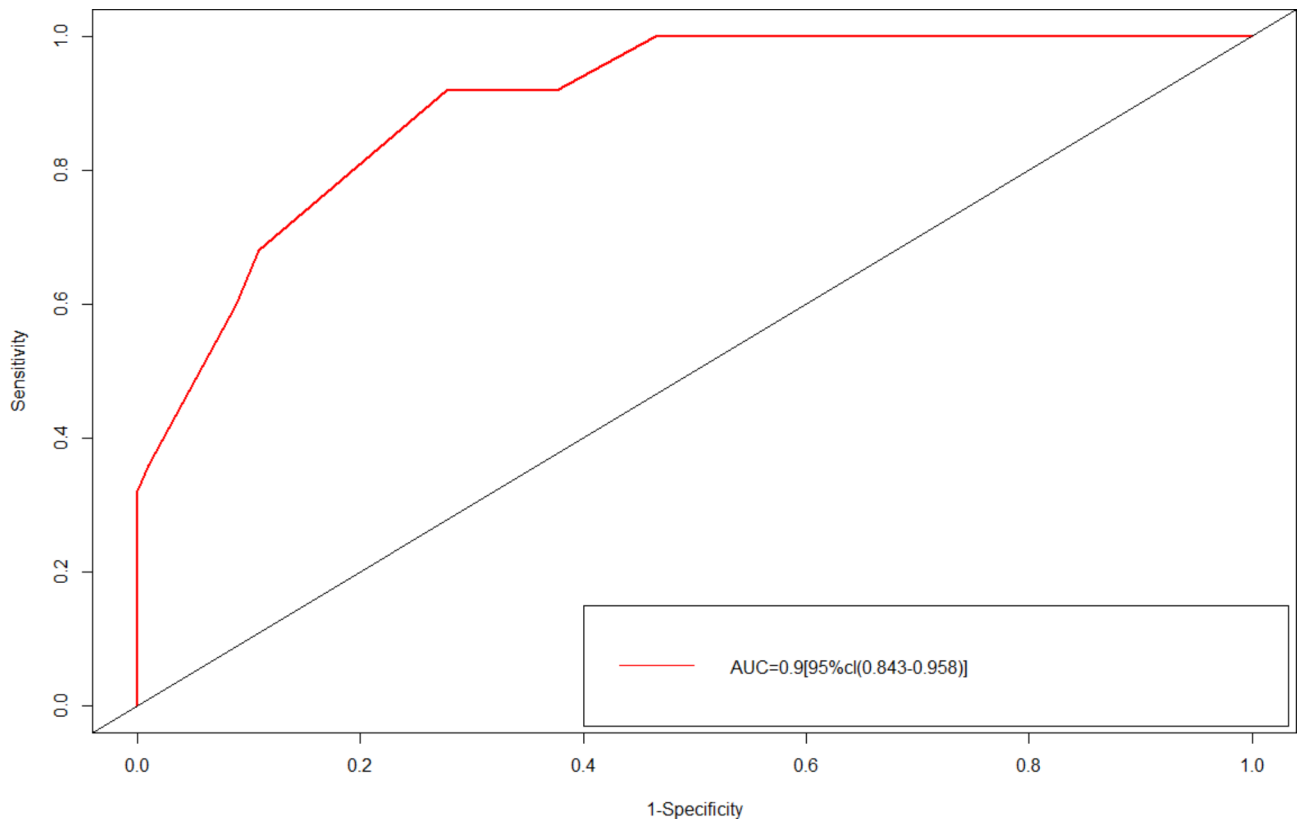


**Fig. 4.** ROC curves of the nomogram prediction model for predicting the recurrence or progression of NFPA in men after transnasal sphenoidal surgery. The area under the ROC curve is 0.9. Abbreviations: NFPA: non-functioning pituitary adenomas; ROC: Receiver Operating Characteristic; AUC: Area Under the Curve.

symptoms. In this study, MRI-related predictors were screened by LASSO regression. The final metric included was the extent of surgical resection, the maximum diameter of the tumour was not included, in addition to the suggestion that early postoperative MRI could help detect tumour recurrence or progression. Based on the column-line graphical model, multiple predictors can be integrated to determine the probability that a patient is not in remission.

Knosp<sup>32</sup> proposed a classical grading of cavernous sinus infiltration based on the relationship between PA and the superior carotid artery (ICA) and intracavernous ICA on MRI. Subsequent studies have found that Knosp classification is not only an important invasive indicator of PA but also plays a crucial role in predicting tumor recurrence<sup>33–35</sup>. In 2015, Micko<sup>18</sup> introduced a revised Knosp classification including the identification of grades 3 A and 3B cavernous sinus ventricular infiltration of the upper or lower cavernous sinus ventricle, which can better predict postoperative remission of PA<sup>35</sup>. Follow-up studies have also shown that patients with Knosp grade 3 A classification usually have higher biochemical remission rates than those with Knosp grades 3B and 4 classification<sup>34,35</sup>. In the present study, only 5% (4/79) of patients with modified Knosp grade 0–3 A tumors experienced recurrence or progression, whereas the rate of recurrence or progression in patients with Knosp grades 3B–4 tumors was 44.6% (21/47), suggesting that the modified Knosp grade is significantly associated with postoperative recurrence or progression and is an independent risk factor that plays an important role.

Ki67 has been described as an independent risk factor for tumor recurrence and progression<sup>10,27</sup>. Petry<sup>36</sup> found that tumors with high Ki-67 expression (> 3%) were more aggressive and had a higher rate of recurrence. Pappy<sup>37</sup> also confirmed that elevated levels of Ki67 ( $\geq 3\%$ ) expression was an important predictor of long-term survival in patients through a retrospective analysis of 501 patients with PA. Moreover, high levels of Ki67 ( $\geq 3\%$ ) were more likely to recur or progress than low levels of Ki67 (< 3%). In patients with recurrence or progression, the Ki67 index after the second surgery was higher than that after the first surgery, possibly due to higher proliferative activity of the residual tumor.

The nomogram can simplify statistical models and estimate the probability of an event (e.g., death or recurrence) with a single value<sup>38</sup>. In addition, the nomogram can integrate multiple prognostic variables and determinants to simulate the complex biological and clinical scenarios of personalized medicine<sup>39</sup>. Although the nomogram has been widely used in predicting recurrence or progression in other tumors<sup>40–42</sup>, a gap exists in the study of nomogram for the recurrence or progression of NFPA in men. Therefore, independent risk factors were integrated to predict the recurrence or progression of NFPA in men after transsphenoidal surgery based on multifactorial analysis.



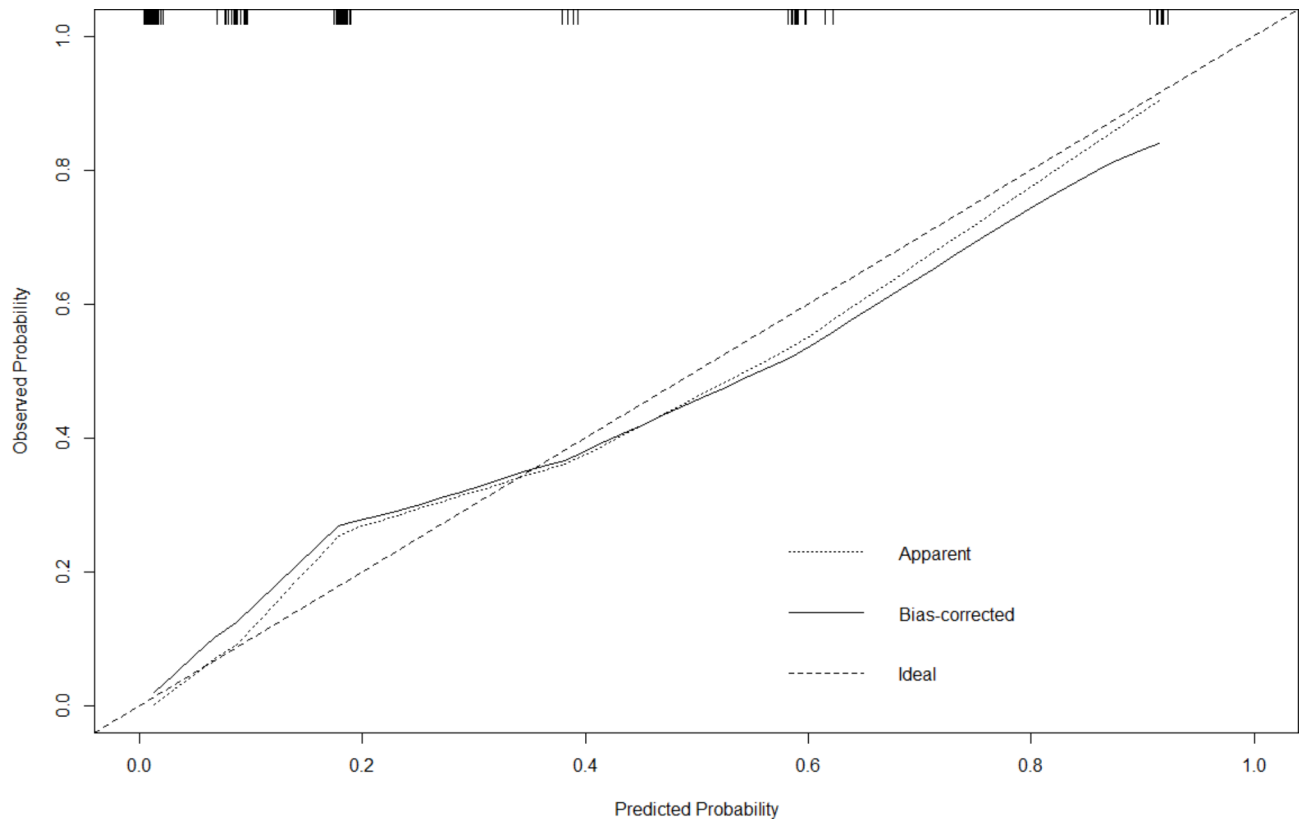


**Fig. 5.** Correction curves for the recurrence or progression of NFPA in men after transnasal sphenoidal surgery in the nomogram prediction model. The x-axis represents the predicted NFPA unmitigated risk. y-axis represents the actual NFPA unmitigated risk. The diagonal dashed line indicates the perfect prediction of the ideal model. The solid line represents the performance of the column plot, where closer to the diagonal dashed line indicates a better prediction. Abbreviations: NFPA: non-functioning pituitary adenomas.

This study had some limitations. First, this was a single-center retrospective study with a small sample size, and some potential predictors were unlikely to reach statistical significance. Further validation of the predictive model in a larger multicenter cohort is needed.

### Conclusion

A nomogram prediction model based on the modified Knosp grading (grades 3B–4), resection extent (partial resection), and Ki-67 ( $\geq 3\%$ ) predicted the recurrence or progression of NFPA in men after transnasal sphenoidal surgery.

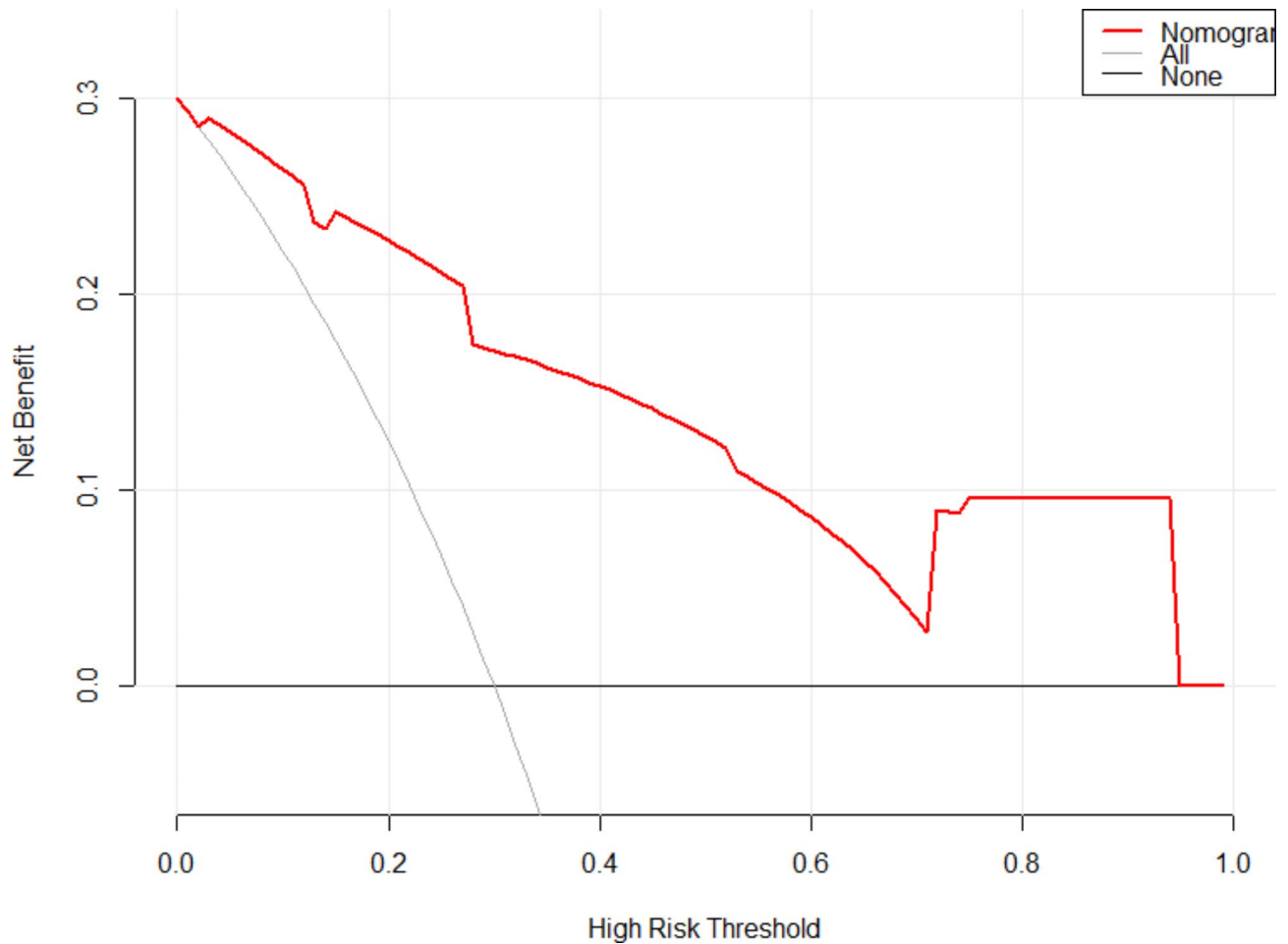


**Fig. 6.** DCA of the nomogram prediction model for predicting the recurrence or progression of NFPA in men after transnasal sphenoidal surgery. The y-axis represents net benefits. The red line represents the nomogram. The thin solid line indicates the assumption that all patients are not in remission. The thick solid line represents the assumption that all patients are in remission. Abbreviations: NFPA: non-functioning pituitary adenomas; DCA: decision curve analysis.

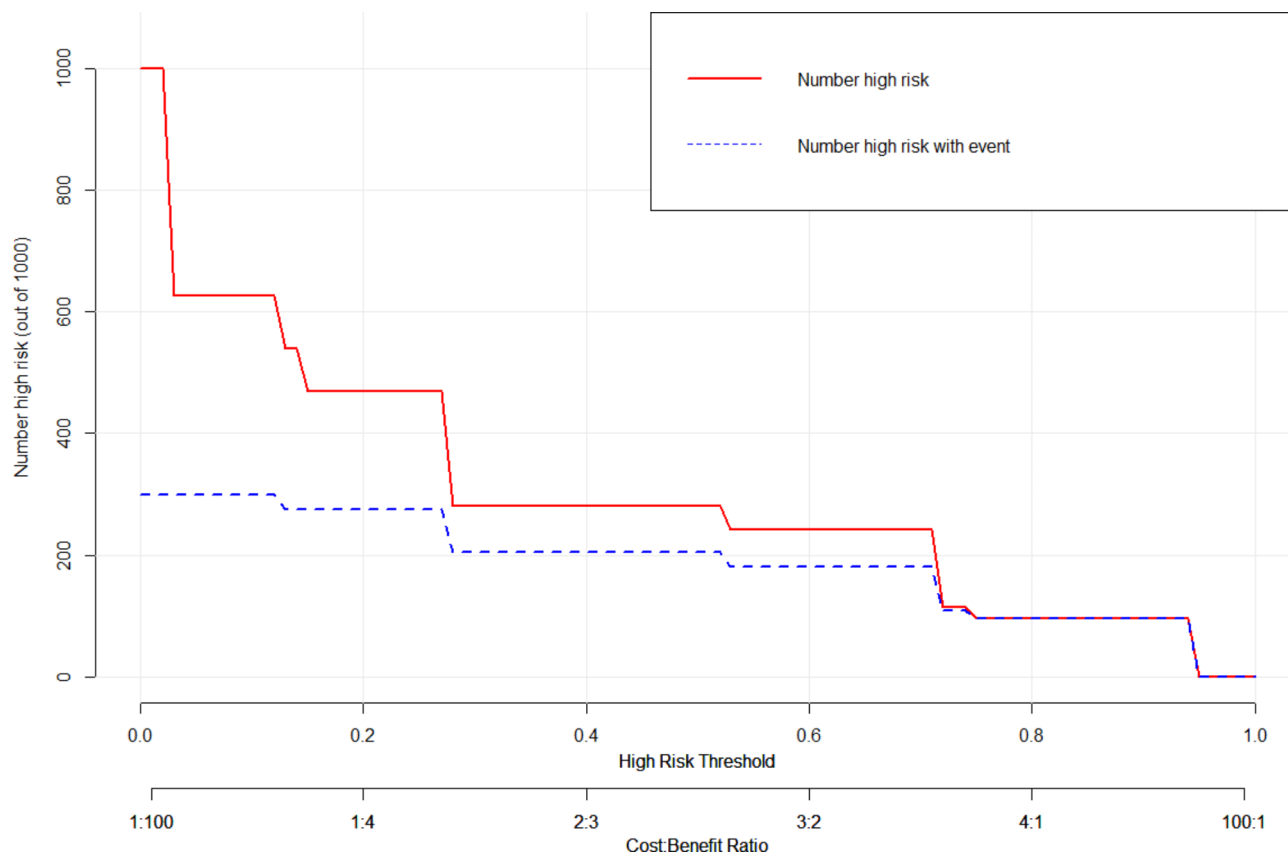


**Fig. 7.** Clinical impact curve (CIC) analyses were performed to assess the clinical applicability of the risk prediction nomogram. The X-axis is the high risk threshold, the Y-axis is the number of people at risk in thousands, the red line represents the number of people predicted by the model to experience the ending event, and the blue line represents the actual number of people. Abbreviations: NFPA: non-functioning pituitary adenomas; DCA: decision curve analysis.

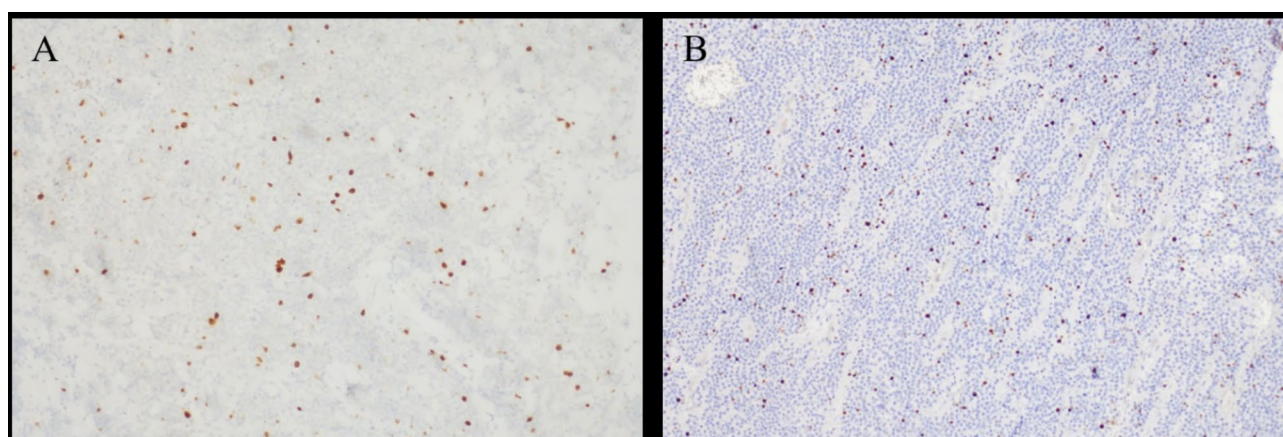


**Fig. 8.** NFPA postoperative Ki67 index (x100): (A) First surgery Ki-67 index 1.68% ( $< 3\%$ ); (B) Second surgery Ki-67 index 3.86% ( $\geq 3\%$  but  $< 20\%$ ). Abbreviations: NFPA: non-functioning pituitary adenomas.

### Data availability

The data that support the findings of this study are available on request from the corresponding author, [Shousen Wang], upon reasonable request.

Received: 26 May 2024; Accepted: 11 September 2024

Published online: 16 September 2024

## References

- Ostrom, Q. T. CBTRUS statistical report: Primary brain and other central nervous system tumors diagnosed in the United States in 2011–2015. *Neuro Oncol.* **20**(suppl\_4), iv1–iv86. <https://doi.org/10.1093/neuonc/nyy131> (2018).
- Rak, B. et al. Pituitary tumours—A large retrospective single-centre study of over 2300 cases. Experience of a tertiary reference centre. *Endokrynol. Pol.* **71**(2), 116–125. <https://doi.org/10.5603/EPa2020.0011> (2020).
- Delgado-López, P. D., Pi-Barrio, J., Dueñas-Polo, M. T., Pascual-Llorente, M. & Gordón-Bolaños, M. C. Recurrent non-functioning pituitary adenomas: A review on the new pathological classification, management guidelines and treatment options. *Clin. Transl. Oncol.* **20**(10), 1233–1245. <https://doi.org/10.1007/s12094-018-1868-6> (2018).
- Margaritopoulos, D. et al. Suprasellar extension independently predicts preoperative pituitary hormone deficiencies in patients with nonfunctioning pituitary macroadenomas: A single-center experience. *Hormones (Athens)*. **19**(2), 245–251. <https://doi.org/10.1007/s42000-020-00183-0> (2020).
- Müslüman, A. M. et al. Surgical results of large and giant pituitary adenomas with special consideration of ophthalmologic outcomes. *World Neurosurg.* **76**(1–2), 141–166. <https://doi.org/10.1016/j.wneu.2011.02.009> (2011).
- Hofstetter, C. P. et al. Volumetric classification of pituitary macroadenomas predicts outcome and morbidity following endoscopic endonasal transsphenoidal surgery. *Pituitary*. **15**(3), 450–463. <https://doi.org/10.1007/s11102-011-0350-z> (2012).
- Juraschka, K. et al. Endoscopic endonasal transsphenoidal approach to large and giant pituitary adenomas: Institutional experience and predictors of extent of resection. *J. Neurosurg.* **121**(1), 75–83. <https://doi.org/10.3171/2014.3.JNS131679> (2014).
- Molitch, M. E. Diagnosis and treatment of pituitary adenomas: A review. *JAMA*. **317**(5), 516–524. <https://doi.org/10.1001/jama.2016.19699> (2017).
- Chen, Y. et al. Natural history of postoperative nonfunctioning pituitary adenomas: A systematic review and meta-analysis. *Neuroendocrinology*. **96**(4), 333–342. <https://doi.org/10.1159/000339823> (2012).
- Reddy, R., Cudlip, S., Byrne, J. V., Karavitaki, N. & Wass, J. A. Can we ever stop imaging in surgically treated and radiotherapy-naïve patients with non-functioning pituitary adenoma?. *Eur. J. Endocrinol.* **165**(5), 739–744. <https://doi.org/10.1530/EJE-11-0566> (2011).
- Dai, Y., Feng, Q. & Huang, J. A nomogram for predicting recurrence of primary hepatocellular carcinoma after resection. *J. Gastrointest. Oncol.* **14**(4), 1900–1901. <https://doi.org/10.21037/jgo-23-138> (2023).
- Ma, Y. N., Zhang, L. X., Hu, Y. Y. & Shi, T. L. Nomogram model for predicting the risk of multidrug-resistant bacteria infection in diabetic foot patients. *Infect. Drug Resist.* **14**, 627–637. <https://doi.org/10.2147/IDR.S287852> (2021).
- Olsson, D. S., Bryngelsson, I. L. & Ragnarsson, O. Higher incidence of morbidity in women than men with non-functioning pituitary adenoma: A Swedish nationwide study. *Eur. J. Endocrinol.* **175**(1), 55–61. <https://doi.org/10.1530/EJE-16-0173> (2016).
- Tampourlou, M., Fountas, A., Ntali, G. & Karavitaki, N. Mortality in patients with non-functioning pituitary adenoma. *Pituitary*. **21**(2), 203–207. <https://doi.org/10.1007/s11102-018-0863-9> (2018).
- Holmes, D. Pituitary gland: Sex difference in comorbidity burden associated with nonfunctioning pituitary adenomas. *Nat. Rev. Endocrinol.* **12**(7), 374. <https://doi.org/10.1038/nrendo.2016.82> (2016).
- Metz, O. & Lopes, M. B. Overview of the 2017 WHO classification of pituitary tumors. *Endocr. Pathol.* **28**(3), 228–243. <https://doi.org/10.1007/s12022-017-9498-z> (2017).
- Šteňo, A. et al. Nonfunctioning pituitary adenomas: Association of Ki-67 and HMGA-1 labeling indices with residual tumor growth. *Acta Neurochir. (Wien)*. **156**(3), 451–461. <https://doi.org/10.1007/s00701-014-1993-0> (2014).
- Miecko, A. S., Wöhrer, A., Wolfsberger, S. & Knosp, E. Invasion of the cavernous sinus space in pituitary adenomas: Endoscopic verification and its correlation with an MRI-based classification. *J. Neurosurg.* **122**(4), 803–811. <https://doi.org/10.3171/2014.12.JNS141083> (2015).
- Hoffman, H. J. Craniopharyngiomas. The role for resection. *Neurosurg. Clin. N. Am.* **1**(1), 173–180 (1990).
- Flores-Rabasa, R. et al. Pre- and post-clinical-radiological and surgical evaluation of patients with pituitary adenoma and metabolic syndrome. *Int. J. Neurosci.* <https://doi.org/10.1080/00207454.2023.2203836> (2023).
- Flesteriu, M., Christ-Crain, M., Langlois, F., Gadelha, M. & Melmed, S. Hypopituitarism. *Lancet*. **403**(10444), 2632–2648. [https://doi.org/10.1016/S0140-6736\(24\)00342-8](https://doi.org/10.1016/S0140-6736(24)00342-8) (2024).
- Trouillas, J. et al. A new prognostic clinicopathological classification of pituitary adenomas: A multicentric case-control study of 410 patients with 8 years post-operative follow-up. *Acta Neuropathol.* **126**(1), 123–135. <https://doi.org/10.1007/s00401-013-1084-y> (2013).
- Roelfsema, F., Biermasz, N. R. & Pereira, A. M. Clinical factors involved in the recurrence of pituitary adenomas after surgical remission: A structured review and meta-analysis. *Pituitary*. **15**(1), 71–83. <https://doi.org/10.1007/s11102-011-0347-7> (2012).
- Lyu, W., Fei, X., Chen, C. & Tang, Y. Nomogram predictive model of post-operative recurrence in non-functioning pituitary adenoma. *Gland Surg.* **10**(2), 807–815. <https://doi.org/10.21037/gs-21-47> (2021).
- Harary, M. et al. Endocrine function and gland volume after endoscopic transsphenoidal surgery for nonfunctional pituitary macroadenomas. *J. Neurosurg.* <https://doi.org/10.3171/2018.5.JNS181054>.
- Osorio, R. C. et al. Socioeconomic predictors of case presentations and outcomes in 225 nonfunctional pituitary adenoma resections. *J. Neurosurg.* <https://doi.org/10.3171/2021.4.JNS21907> (2021).
- Tampourlou, M. et al. Outcome of nonfunctioning pituitary adenomas that regrow after primary treatment: A study from two large UK centers. *J. Clin. Endocrinol. Metab.* **102**(6), 1889–1897. <https://doi.org/10.1210/je.2016-4061> (2017).
- Greenman, Y. et al. Postoperative surveillance of clinically nonfunctioning pituitary macroadenomas: Markers of tumour quiescence and regrowth. *Clin. Endocrinol. (Oxf)*. **58**(6), 763–769. <https://doi.org/10.1046/j.1365-2265.2003.01784.x> (2003).
- Kristof, R. A. et al. Endocrinological outcome following first time transsphenoidal surgery for GH-, ACTH-, and PRL-secreting pituitary adenomas. *Acta Neurochir. (Wien)*. **144**(6), 555–561. <https://doi.org/10.1007/s00701-002-0938-1> (2002).
- Lelotte, J. et al. Both invasiveness and proliferation criteria predict recurrence of non-functioning pituitary macroadenomas after surgery: A retrospective analysis of a monocentric cohort of 120 patients. *Eur. J. Endocrinol.* **178**(3), 237–246. <https://doi.org/10.1530/EJE-17-0965> (2018).
- Chang, E. F. et al. Long term outcome following repeat transsphenoidal surgery for recurrent endocrine-inactive pituitary adenomas. *Pituitary*. **13**(3), 223–229. <https://doi.org/10.1007/s11102-010-0221-z> (2010).
- Knosp, E., Steiner, E., Kitz, K. & Matula, C. Pituitary adenomas with invasion of the cavernous sinus space: A magnetic resonance imaging classification compared with surgical findings. *Neurosurgery*. **33**(4), 610–618. <https://doi.org/10.1227/00006123-199310000-00008> (1993).
- Buchy, M. et al. Predicting early post-operative remission in pituitary adenomas: Evaluation of the modified knosp classification. *Pituitary*. **22**(5), 467–475. <https://doi.org/10.1007/s11102-019-00976-6> (2019).
- Araujo-Castro, M. et al. Predictive model of surgical remission in acromegaly: Age, presurgical GH levels and Knosp grade as the best predictors of surgical remission. *J. Endocrinol. Invest.* **44**(1), 183–193. <https://doi.org/10.1007/s40618-020-01296-4> (2021).
- Yuhan, L., Zhiqun, W., Jihui, T. & Renlong, P. Ki-67 labeling index and Knosp classification of pituitary adenomas. *Br. J. Neurosurg.* **38**(2), 393–397. <https://doi.org/10.1080/02688697.2021.1884186> (2024).
- Petry, C. et al. Evaluation of the potential of the Ki67 index to predict tumor evolution in patients with pituitary adenoma. *Int. J. Clin. Exp. Pathol.* **12**(1), 320–326 (2019).
- Pappy, A. L. 2nd. et al. Predictive modeling for pituitary adenomas: Single center experience in 501 consecutive patients. *Pituitary*. **22**(5), 520–531. <https://doi.org/10.1007/s11102-019-00982-8> (2019).

38. Iasonos, A., Schrag, D., Raj, G. V. & Panageas, K. S. How to build and interpret a nomogram for cancer prognosis. *J. Clin. Oncol.* **26**(8), 1364–1370. <https://doi.org/10.1200/JCO.2007.12.9791> (2008).
39. Balachandran, V. P., Gonen, M., Smith, J. J. & DeMatteo, R. P. Nomograms in oncology: More than meets the eye. *Lancet Oncol.* **16**(4), e173–e180. [https://doi.org/10.1016/S1470-2045\(14\)71116-7](https://doi.org/10.1016/S1470-2045(14)71116-7) (2015).
40. Huang, R., Kong, Y., Luo, Z. & Li, Q. LncRNA NDUFA6-DT: A comprehensive analysis of a potential LncRNA biomarker and its regulatory mechanisms in gliomas. *Genes (Basel)*. **15**(4), 483. <https://doi.org/10.3390/genes15040483> (2024).
41. Mokbel, S. et al. Development and validation of an inflammatory prognostic index to predict outcomes in advanced/metastatic urothelial cancer patients receiving immune checkpoint inhibitors. *Cancers (Basel)*. **16**(8), 1465. <https://doi.org/10.3390/cancers16081465> (2024).
42. Ren, L. et al. Crosstalk of disulfidptosis-related subtypes identifying a prognostic signature to improve prognosis and immunotherapy responses of clear cell renal cell carcinoma patients. *BMC Genomics*. **25**(1), 413. <https://doi.org/10.1186/s12864-024-10307-0> (2024).

## Acknowledgements

Jiansheng Zhong and Yuyang Chen contributed equally to this paper and are listed as first coauthors. The authors thank the Joint Logistics Medical Key Specialty Project (LQZD-SW) and the Fujian Provincial Science and Technology Program Science and Technology Innovation Platform Project (2022Y2017).

## Author contributions

Jiansheng Zhong: Data curation, Writing- Original draft preparation. Yuyang Chen: Data curation, Writing- Original draft preparation. Mingyue Wang: Investigation and Supervision. Jun Li: Supervision. Ziqi Li: Supervision. Haixiang Li: Investigation. Liangfeng Wei: Formal analysis, Validation. Shousen Wang: Writing- Reviewing and Editing, Supervision. (Notes: Jiansheng Zhong and Yuyang Chen contributed equally to this paper and are listed as first coauthors).

## Declarations

### Competing interests

The authors declare no competing interests.

## Additional information

**Supplementary Information** The online version contains supplementary material available at <https://doi.org/10.1038/s41598-024-72944-5>.

**Correspondence** and requests for materials should be addressed to S.W.

**Reprints and permissions information** is available at [www.nature.com/reprints](http://www.nature.com/reprints).

**Publisher's note** Springer Nature remains neutral with regard to jurisdictional claims in published maps and institutional affiliations.

**Open Access** This article is licensed under a Creative Commons Attribution-NonCommercial-NoDerivatives 4.0 International License, which permits any non-commercial use, sharing, distribution and reproduction in any medium or format, as long as you give appropriate credit to the original author(s) and the source, provide a link to the Creative Commons licence, and indicate if you modified the licensed material. You do not have permission under this licence to share adapted material derived from this article or parts of it. The images or other third party material in this article are included in the article's Creative Commons licence, unless indicated otherwise in a credit line to the material. If material is not included in the article's Creative Commons licence and your intended use is not permitted by statutory regulation or exceeds the permitted use, you will need to obtain permission directly from the copyright holder. To view a copy of this licence, visit <http://creativecommons.org/licenses/by-nc-nd/4.0/>.

© The Author(s) 2024